Accepted Manuscript

Study of the tribological properties and ageing of alkyphosphonic acid films on galvanized steel

Donald Hill, Peter J. Holliman, James McGettrick, Marco Appelman, Pranesh Chatterjee, Trystan M. Watson, David Worsley

PII: S0301-679X(17)30530-3

DOI: 10.1016/j.triboint.2017.11.015

Reference: JTRI 4955

To appear in: *Tribology International*

Received Date: 15 May 2017

Revised Date: 8 November 2017

Accepted Date: 9 November 2017

Please cite this article as: Hill D, Holliman PJ, McGettrick J, Appelman M, Chatterjee P, Watson TM, Worsley D, Study of the tribological properties and ageing of alkyphosphonic acid films on galvanized steel, *Tribology International* (2017), doi: 10.1016/j.triboint.2017.11.015.

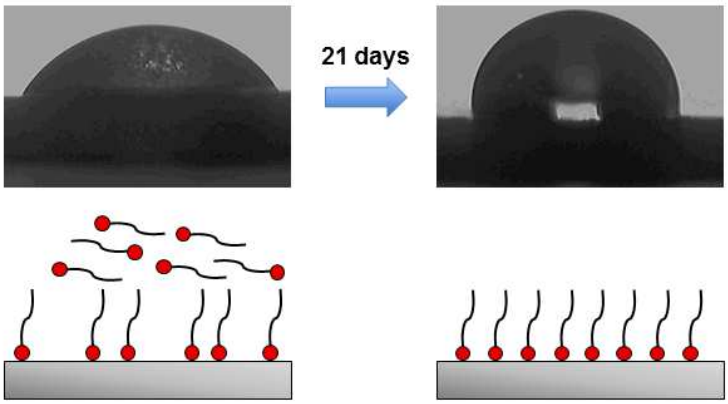

Donald Hill[a], Peter J. Holliman[a,*], James McGettrick[a], Marco Appelman[b], Pranesh Chatterjee[b], Trystan M. Watson[a] and David Worsley[a]

[a] College of Engineering, Bay Campus, Swansea University, Swansea, SA1 8EN, UK

[b] Tata Steel Research & Development, PO Box 10000, 1970 CA Ijmuiden

* corresponding author. E-mail address: p.j.holliman@swansea.ac.uk

Abstract

The tribological properties of octyl-, dodecyl- or octadecylphosphonic acid coatings on TiO_2-coated galvanized steel substrates have been studied using linear friction testing (LFT) as potential lubricants for deep drawing automotive steels. LFT data show that the coatings reduce the coefficient of friction by > 65% from 0.31 to < 0.11. Confocal microscopy reveals that phosphonate-coated surfaces suffer considerably less wear than uncoated substrates during LFT. Water contact angle (WCA), XPS and IR data show that physisorbed phosphonates are removed by acetone washing leaving chemisorbed material. Data from a month-long ageing study using WCA, XPS and IR data shows that most of the physisorbed phosphonates become chemisorbed with time increasing hydrophobicity and tribological properties of the surfaces. Most of the changes occur within 14 days of coating and, after 21 days, no further surface changes were observed.

Keywords: automotive steel, forming, low friction, phosphonic acids.

1. Introduction

pressure that carries the load [3, 4]. By reducing frictional forces, the oils ensure that the parts produced are free from visible signs of wear. However, surface texture is required to hold the oil in place during forming [4]. This limits the steel that can be used because smoother surfaces, which might be preferable for automotive products, cannot retain sufficient lubricant. In addition, drawing oils are also often used in tandem with anti-wear additives that are harmful to the environment [5].

Functionalization of interfaces with self-assembled monolayers (SAMs) has attracted interest in recent years for various uses [6-9] including as lubricants in micro/nanoelectromechanical systems [6]. In general, molecules that spontaneously form SAMs contain a head group to chemically bind to surface atoms (e.g. a thiol, carboxylate or silyl group [8, 9]), a spacer (e.g. a hydro- or fluorocarbon chain) and a terminal group that forms the outer surface [6]. Lubricating SAMs are believed to act like molecular springs or brushes during tribological contact, where multiple, orientated spacer chains act together to lower shear forces at the interface [10-12]. Recently, we have reported the use of carboxylate-linked SAMs as coatings in sheet metal forming processes as an alternative to oil-based lubricants because their mechanism of action not being dependent on the surface topography, and also the potential for lower environmental impact of alkyl carboxylate SAMs [13]. By comparison, to the best of our knowledge, alkylphosphonic acids of the type $RPO(OH)_2$, where R is an alkyl group, have not been studied as lubricant SAMs on steel surfaces. However, the phosphonate moiety is known to form three bonds with surface sites on various different metal oxides [14-16]. This should result in stronger SAM:substrate interfacial bonds but should also influence the orientation of the alkyl chains above the substrate surface. These factors should influence the wear performance during the high pressures encountered in

of substrates using sol-gel methods [17-19] similar to those used to fabricate electron capture layers in solar cells [20].

In this study, we have studied octyl-, dodecyl-, and octadecylphosphonic acids (labelled here as **R8-P**, **R12-P** and **R18-P**, respectively) formed on TiO_2-coated galvanized steel substrates. We have studied their tribological properties using Linear Friction Testing (LFT) and wear resistance using confocal microscopy. These data have been correlated with detailed surface characterization using water contact angle (WCA), IR, XPS and thermal analysis studies to understand the performance of "as prepared" and aged coatings. In a related study, Roizard *et al.* have investigated the sliding of ferritic stainless steel against steel ball bearings, lubricated with alkylphosphonic acids in an alcoholic solution [21]. Here, they ascribed the reduction in friction to be due to the formation of a tribofilm consisting of the alkylphosphonic acids. In this paper, we ascribe the reduction in friction to be due to the presence of thin films formed from alkylphosphonic acids on the surfaces of metal sheets.

2. Experimental

2.1 Samples and chemicals

A low carbon, formable strip steel (DX56, Tata Steel) was cut into 50×300 mm strips for LFT and wear studies, and into 10×20 mm coupons for characterization (for composition, see S1). Prior to testing, surface oil was removed by scrubbing with water and detergent, air-drying, and ultra-sonicating in acetone for 5 min. All other chemicals were obtained from Sigma Aldrich and used without further purification.

2.2 Surface functionalization and characterization

analysis. Selected samples were also acetone rinsed for 5 min.

For materials characterization, coefficients of friction (μ) were measured using an LFT method based on Trzepiecinski *et al.* [22] using an in-house constructed instrument at Tata Steel, IJmuiden at 22-24^{o}C and 30-45% RH as described by Hill *et al.* [13] (full details are given in S2). Confocal micrographs were imaged with a Nanofocus μSurf Mobile at 20x magnification using a 2.1x2.1 mm field of view. Data were plotted using Mountains software, v. 7.3. Static water contact angles (WCA) were measured using DI water (n = 5, 5μl droplets) with a USB 2.0 camera with attached goniometer. Data were fitted using FTA 32 software (FTA 32 Europe Ltd). Infrared spectra (650 and 4000cm^{-1}, 4 scans, 4 cm^{-1} resolution) were recorded on a Perkin Elmer 100 Series ATR-FTIR spectrometer. Scanning Electron Microscopy (SEM) was carried out on a Hitachi S4800 field emission gun (FEG)-SEM at 1.0kV and 5μA, and a working distance of 11.5mm. Energy Dispersive X-Ray (EDX) spectra were acquired at 15.0kV and 15μA for 100 s on 5 different areas with a Silicon Drift X-Max EDX detector and Inca EDX software (Oxford Instr.). X-ray photoelectron spectra (XPS) were recorded on an Axis Supra XPS using a monochromated Al K_{α} source and large area slot mode detector (300x800μm analysis area). Data were recorded using a charge neutralizer to limit differential charging and binding energies were calibrated to the main hydrocarbon peak (BE 284.8 eV). Survey scans were performed using a pass energy of 160eV and high resolution spectra were recorded using a 0.1 eV step size and a pass energy of 20 eV. Data were fitted using CASA software with Shirley backgrounds. Thermal analysis samples were prepared by stirring 300 mg of P25 TiO_2 powder (Degussa) in 100 mM isopropanolic solution of **R12-P** at 25 ^{o}C for 24 h followed by centrifugation at 2000 rpm for 5 min. The supernatant was decanted and the powder dried at 50 ^{o}C for 30 min. Thermal gravimetric analysis (TGA)

3. Results and Discussion

3.1 Linear Friction Testing (LFT) and Confocal Microscopy

LFT measures the coefficient of friction (μ). It is a technique designed to simulate the conditions encountered during deep drawing of automotive steels and involves high pressure contacts formed between the tools and the substrate. Values for μ of pristine and TiO_2-coated DX56 substrates vary inconsistently along the sample length (Fig. 1a), which is ascribed to varying surface roughness. The samples also show evidence of static friction with spikes in the μ between 0 and 5 mm. The mean μ of DX56 is 0.309 ± 0.052 (Fig. 1b) with similar values recorded after $Ti(OiPr)_4$ treatment and/or acetone rinsing, suggesting that TiO_2 does not imbue any lubricity onto the substrate.

By comparison, the μ of all the alkylphosphonic acid coatings is consistent between different alkyl chain lengths (**R8-P** to **R18-P**) whilst also being substantially lower (0.074 to 0.109) than the DX56 or TiO_2-coated DX56 and much more consistent along the sample length suggesting far less static friction for these materials. Between the different alkyl chain lengths, the μ of the **R8-P** and **R18-P** coatings are slightly higher (0.104 ± 0.004 and 0.109 ± 0.005, respectively) than the **R12-P** (0.074 ± 0.001), which may reflect the lower surface coverage for the **R8-P** and **R18-P** molecules (see XPS data).

Interestingly, there is a slight increase in μ for all phosphonate coatings after acetone rinsing with the biggest increase for the **R12-P** coating where μ increases from 0.074 ± 0.001 to 0.112 ± 0.011. These changes in μ are consistent with previous reports for alkyl phosphonic acid monolayers on copper surfaces [4, 23]. This is ascribed to two main factors. Firstly, prior to acetone rinsing, multilayers of physisorbed alkylphosphonic acids act as barrier coatings, reducing the frictional force through blocking contact between surface asperities. However,

the data show that the acetone-washed surfaces show similar frictional behaviour, regardless of the spacer chain length. In agreement with these data, previous studies have shown that the stabilization energy incurred through increasing the number of methylene (CH_2) groups in a chain saturates between n = 8-10, where n is the number of carbon atoms [23]. Consequently, this could mean that the packing densities of the chemisorbed alkylphosphonic acids could be similar, and this could be responsible for the similar tribological behaviour. For these coatings to affect lubricity, the phosphonate packing densities must be high enough to arrange the alkyl chains close enough together so that the combined inter-chain interactions (e.g. van der Waals forces) are great enough to influence lubricity. Additionally, the μ or WCA measurements are effectively averaged values resulting from much wider length scales (i.e. μm to cm) compared to packing densities (i.e. Å to nm). Thus, for the **R8-P**, **R12-P** and **R18-P** molecules, these data suggest that the combined influence of packing densities and inter-chain interactions averaged out over the much longer lengths scales are sufficiently similar that they result in identical tribological behaviour.

3.2 Confocal and Scanning Electron Microscopy

Fig. 2 shows wear analysis data after single pass LFT measurements using confocal microscopy for DX56, TiO_2-coated DX56 and an **R12-P** coated substrate. The data show that DX56 and TiO_2-coated substrates suffer deep scratches, which are ascribed to galling phenomena [25]. We ascribe this galling to the removal of particles from the zinc-rich galvanic layer, which forms the outermost surface of uncoated DX56 by stick/slip wear. The zinc particles become trapped between the LFT tool and the substrate and friction-derived heat adheres the particles to the LFT tool (Fig. 3) and work hardens them as described by van

18P coated substrates (Fig. 2c and S21), indicative of reduced galling. Instead, the confocal data suggest that, if material is removed from the surface of **R12-P** or **R18-P** treated substrates, then that material is removed in a more consistent/even manner. To fully illustrate this, detailed confocal data and analysis for the uncoated DX56 and the **R8-P**, **R12-P** and **R18-P** samples before and after ten LFT passes has been carried out. Fig. 2d shows the cross - sectional data whilst the complete set of data are shown in S14-S21. As an example, this is shown particularly clearly when considering the average surface roughness and cross-sectional line profile of the **R18-P** coating before and after LFT testing where R_a drops from 3.1 μm to 0.42μm after 10 LFT passes (S20 - d, e, g *versus* S21 - d, e, g). For this sample, the confocal data suggest that the surface is smoothed by LFT treatment whereby the action of the LFT tool is to abrade the higher peaks on the substrate in an even manner without any galling. In line with this, small amounts of zinc from the substrate surface are observed on the LFT tool for R18-P (S21f).

Further analysis of multi-pass LFT data (10 LFT passes) for the **R12-P** coating before and after acetone rinsing *versus* uncoated DX56 (Fig.3 and S13) shows that the μ of the uncoated DX56 increases to values > 0.40 after *ca.* five passes before increasing further to > 0.50 after 10 LFT passes. Large zinc flakes were observed on the surface of the tools (Fig. 3bii, S15f), indicative of the extreme galling initiated by the high friction contacts made between the substrate and the surface of the tools.

Comparing the other samples, S13 shows the μ data of all the alkylphosphonates remains <0.10 up to 4 LFT passes before the value for R8-P value increases to *ca.* 0.20. In contrast, the μ data of unrinsed **R12-P** and R18-p coatings remain relatively constant (*ca.* 0.05) for all 10 LFT passes (S13). Less zinc is observed on the LFT flat tools for **R12-P** and

Interestingly, we anticipate there being both chemi- and physisorbed **R12-P** or **R18-P** being present on these respective surfaces. There are two possibilities here; firstly, that physisorbed phosphonates coat the surface of the LFT tool as well as the substrate. This would extend the influence of these two phosphonate coatings on the LFT data. A second possibility is that, for **R12-P** and **R18-P**, the physisorbed phosphonates act in a "self-healing" manner and, as phosphonate-coated zinc is removed from the surface, this unbound phosphonate material is spread across the fresh surface; effectively to imbue fresh lubricity.

In contrast, the μ of acetone-rinsed **R12-P** coatings increases after *ca.* 5 passes from *ca.* 0.07 to 0.12-0.15, suggesting that coating material is removed by the tribological contact. After 10 LFT passes, μ is > 0.20, which is closer to the value for single pass LFT on uncoated DX56. In explanation of these data, IR data show that the acetone-rinsed samples consist predominantly of chemisorbed **R12-P**; i.e. molecules chemical bound to the outermost surface of the galvanized surface. Then, during the LFT measurements, removal of surface zinc particles will inevitably also remove any **R12-P** molecules attached to these. In fact, the data suggest that the majority of **R12-P** has been removed which suggests that the majority of the outer surface of zinc has also been removed from this sample causing the increase in friction.

In support of these assertions, confocal micrographs taken of uncoated DX56 (Fig. 3c) reveal that 10 LFT passes leads to delamination of the large amounts of the zinc coating in discrete areas. Confocal microscopy of the **R12-P** substrate (Fig. 3d) after 10 LFT passes shows that the surface topography becomes smoother as a result of multiple LFT passes. In addition, fewer scratches are observed indicating that less wear to the surface had occurred. In contrast, the acetone-rinsed **R12-P** substrate (Fig. 3e) shows more surface scratches. This

which are ascribed to an inhomogeneous TiO_2 coating which contains some agglomerates. Variable titanium signals in the EDX spectra (S6b and c) confirm this. The SEM micrographs of the phosphonic acid coatings measured using a 1.0 kV accelerating voltage show clear evidence of additional surface material (S5c-e). However, the thickness or composition of the surface coating appears to vary across the substrate surface as evidenced by lighter and darker regions particularly on the **R8-P** and **R12-P** samples which suggests differential charging from the electron beam is taking place at different places on the surface. The **R12-P** shows very clear deposits of surface material which is consistent with multi-layer deposition because a monolayer coverage would not be visible at the resolution possible using SEM. EDX data have also been measured for these samples but at a 15.0 kV accelerating voltage. Whilst this will more fully excite the surface atoms to enhance the limit of EDX detection, it comes at the expense of an increased electron beam penetration depth which can damage surface layers and reduce surface sensitivity. Hence, the SEM images look different from the FEG-SEM data measured at 1.0 kV accelerating voltage. For the R8-P coating (S6d), whilst peaks for Ti at 4.5-5.0 keV do vary across the surface, the P peak at 2.1 keV is present in all EDX spectra. By comparison, whilst the **R12-P** EDX data show a similar, slight variance in the Ti peaks from weak signals to no observable Ti peaks, the P peak varies from below the detection limit to off scale indicating some areas with multi-layer coverage and other areas with little or no **R12-P** coating. Finally, the **R18-P** sample is more similar to the **R8-P** coating in that the Ti peaks vary from weak to below the detection limit. However, there is a more consistent if lower P signal across the sample suggesting a more consistent coverage but with a lower loading than **R8-P** or **R12-P**.

ZnSe ATR crystal. After deposition of the alkylphosphonic acids, the IR spectra show bands coincident with the neat alkylphosphonic acids suggesting that the coatings were largely composed of physisorbed **R8-P**, **R12-P** and **R18-P** (spectra and full assignments according to [4, 23, 26] are in S7).

Using **R12-P** as a model, samples were aged under ambient conditions in air. After 3 days, the υ P=O band at 1230 cm^{-1} disappears and a new broad peak is observed at *ca.* 1080 cm^{-1} which is ascribed to O-P-O asymmetric stretching (Fig. 4). This suggests that phosphonates linked either through bidentate bonding to the surface and/or physisorbed material becomes chemisorbed to surface sites in tridentate coordination mode. This bonding mode is in line with previous studies [4, 22]. After 7 days, the O-P-O asymmetric stretch narrows and shifts to *ca.* 1070 cm^{-1}. In addition, a weak band appears at *ca.* 1154 cm^{-1}, which is ascribed to a symmetric stretch of chemisorbed **R12-P**. No further changes in the IR spectra of the **R12-P** samples is observed after 14 days or 21 days of ageing including acetone-washed samples. This suggests that all the phosphonates have re-ordered themselves into chemisorbed, tridentate coordination, which is resistant to solvent rinsing, in line with previously reported data [4]. By comparison, unaged samples show no phosphonate bands after acetone washing in line with the removal of physisorbed material.

3.4 X-ray Photoelectron Spectroscopy (XPS) and Thermogravimetric analysis (TGA)

The XP data of uncoated DX56 are in agreement with previous reports showing Zn $2p_{1/2}$ and $2p_{3/2}$ peaks (1021.2 and 1044.0 eV), an Al 2p peak (73.9 eV) and a broad O 1s peak for surface oxide at 531.70 eV [27-29] (S8). Following the $Ti(OiPr)_4$ treatment, Ti $2p_{1/2}$ and $2p_{3/2}$

190.8 and 132.8 eV [4, 33] (S10, S11). Atomic concentrations show that the coated surfaces are carbonaceous with only weak Zn peaks (e.g. 1.6 ± 0.3%, zero and 0.2 ± 0.1% Zn for **R8-P**, **R12-P** and **R18-P**, respectively). Since it is known that the mean free path escape depths for typical photoelectron kinetic energies (10-1000eV) are 1-10 nm [34], this suggests multiple layers of alkylphosphonic acids are present. However, the observation of Ti 2p peaks in all the phosphonate-coated samples suggests that the phosphonates may deposit in thicker layers on Zn-rich areas; i.e. areas not covered by TiO_2.

More intense Zn and Ti peaks are then observed for acetone rinsed **R12-P** and **R18-P** coatings in line with removal of physisorbed alkylphosphonic acids. In line with this, weaker P 2s and 2p peaks are also observed. By comparison, the **R8-P** coating shows similar atomic concentrations of Zn and Ti (1.6 ± 0.3% and 1.2 ± 0.3%, respectively) before and after rinsing whilst the P signal drops from 6.7 ± 0.2% to 5.9%. This suggests that there may be areas of surface not coated by **R8-P** and also that acetone removes less physisorbed **R8-P** from the surface compared to **R12-P** or **R18-P**.

To further investigate phosphonate loading on TiO_2 surfaces, **R12-P** was first sorbed onto Degussa P25 powder and then analysed by TGA. The data show a mass loss of 5.6% for **R12-P**, which drops to 4.6% after acetone rinsing (S12) compared to 0.5% mass loss for a control sample of untreated P25. This confirms that **R12-P** material is removed by acetone washing in line with the IR and XPS data.

The effect of ageing on the **R12-P** coating has also been studied (Fig. 5). Thus, for “as prepared” samples, no Zn 3s peak is observed and only the P 2p peak is seen (Fig. 5a). However, when this sample is immediately washed with acetone, the ratio of the areas of the P 2p peak to Zn 3s peaks is 3.1 to 1.0. However, after 10 days ageing, this ratio after acetone

3.5 Water contact angle (WCA) measurements

Following cleaning, the WCA of the DX56 steel substrate was measured to be 54 ± 5^{o} (Fig. 6). Within experimental error, this did not change after TiO_2 coating. In addition, acetone rinsing either the uncoated or TiO_2-coated DX56 substrate did not change the WCA data. Functionalizing TiO_2-coated DX56 substrates with **R8-P** or **R18-P** generated more hydrophobic surfaces (112 ± 7^{o} and 91± 7^{o}, respectively). Whilst the WCA of **R8-P** did not change on acetone rinsing, the **R18-P** coating became more hydrophobic after acetone rinsing (110 ± 4^{o}). By comparison, the WCA of the **R12-P** coating is slightly more hydrophilic (47± 5^{o}) than the uncoated or TiO_2 coated DX56 substrate but this value increases to 114 ± 7^{o} after acetone rinsing. The absence of any Zn 3s peak in the "as deposited sample (Fig. 5a) suggests that more than a monolayer of **R12-P** is initially deposited. Because, in a multi-layer surface there are no surface sites available for the phosphonate linker groups, some will orient themselves away from the surface. The charged nature of these groups will inevitably reduce surface tension with the water droplet, which will reduce the WCA. However, acetone rinsing will remove excess, physisorbed **R12-P** or **R18-P** leaving an outer surface dominated by alkyl groups from chemisorbed phosphonates resulting in a more coherently hydrophobic surface. Such increases in WCAs after acetone rinsing are similar to those observed for alkylphosphonic acids on copper [4] and aluminium [35], carboxylic acids on mica [36], and alkylthiols on gold [37].

The wettability of aged **R12-P** coated substrates has also been investigated. From an initial value of 47± 5^{o}, the WCA increased to 84 ± 10^{o} (after 3 days), to 96 ± 11^{o} (after 7 days) and to 103 ± 4^{o} after 21d. The changing WCA suggests surface rearrangement of the

ambient conditions (kT being *ca.* 2.5 kJ mol^{-1} at 25°C), which allows physisorbed material to diffuse across the surface to chemisorb to vacant surface sites. After 21 days ageing, within experimental error, the WCA did not vary after acetone rinsing. This suggests that whatever physisorbed material is present has had sufficient time to chemisorb and fill any vacant sites. Thus, whatever physisorbed material is removed by acetone washing leaves behind a surface with a homogeneous array of alkyl groups oriented perpendicular to the surface.

To test how wear might affect WCA, a sample of DX56 was cleaned and the WCA found to be 64.0° ± 11.5°. After R12P had been deposited on this substrate, the WCA dropped to 50.8° ± 5.6° in line with other data for unaged samples. This surface was then polished using an Al_2O_3/water slurry abrasive to simulate wear and water the WCA of the surface changed to 68.1° ± 4.8°. This is similar to the WCA of uncoated DX56 substrate and is in line with the removal of physisorbed R12P by abrasion.

4. Conclusions

Our data show that phosphonic acids with alkyl chain lengths ranging from octyl to octadecyl (**R8-P**, **R12-P** and **R18-P**) rapidly deposit from solution onto TiO_2-coated galvanized steel substrates as chemi- and physisorbed species. The as-deposited **R8-P**, **R12-P** and **R18-P** coatings lower substrate coefficients of friction (μ) and so increase lubricity relative to uncoated DX56 substrate. Whilst acetone washing removes physisorbed phosphonates and increases μ, leaving unwashed substrates to age under ambient conditions results in surface reorganization whereby IR and XPS data show that material becomes chemisorbed which increases WCA and lowers the μ. These data show that the surface loading and bonding of the phosphonates both influence lubricity. Furthermore, the negative correlation between WCA

microscopy also confirms considerably less wear on phosphonate-coated samples making this approach a promising candidate for inducing inherent lubricity in sheet metal forming processes like deep drawing.

Acknowledgements

We gratefully acknowledge funding from EPSRC EngD and Tata Steel (DH), the Welsh Government for Sêr Cymru (PJH) and EPSRC/InnovateUK for SPECIFIC IKC funding EP/I019278/1 (JMc).

References

[1] Allen SJ, Mahdavian SM. The effect of lubrication on die expansion during the deep drawing of axisymmetrical steel cups, J. Mater. Process. Tech. 2008;199:102–107.

[2] Altan T, Tekkaya AE. Sheet Metal Forming: Fundamentals, Ed. Altan T, Tekkaya AE, ASM Int., Ohio; 2012, Chap. 2: p. 15-16.

[3] Karupannasamy DK, Hol J, de Rooij MB, Meinders T, Schipper DJ. Modelling mixed lubrication for deep drawing processes, Wear 2012;294-295:296-304.

[4] Moine MM, Roizard X, Melot JM, Carpientier L, Cornuaault PH, Lallemand F, Rauch JM, Heintz O, Lallemand S. Grafting and characterization of dodecylphosphonic acid on copper: macro-tribological behavior and surface properties, Surface Coatings Tech. 2013;232:567-574.

[5] de Rooij M. Tribological aspects of unlubricated deep drawing processes, PhD thesis, University of Twente; 1998, Chap. 1: 2-3.

[6] Chaki NK, Vijayamohanan K. Self-assembled monolayers as a tunable platform for biosensor applications, Biosensors and Bioelectronics 2002;17:1-12.

[9] Cheng H, Hu Y. Influence of chain ordering on frictional properties of self-assembled monolayers (SAMs) in nanolubrication, Adv. Colloid Interface Sci. 2012;171-172:53-65.

[10] Liu H, Bhushan B, Investigation of nanotribological properties of self-assembled monolayers with alkyl and biphenyl spacer chains, Ultramicroscopy 2002;91:185-202.

[11] Siepmann JI, McDonald IR. Monte Carlo simulation of the mechanical relaxation of a self-assembled monolayer, Phys. Rev, Letters 1993;70:453-456.

[12] Maege I, Jaehne E, Henke A, Adler HJP, Bram C, Jung C, Stratmann M. Self-assembling adhesion promoters for corrosion resistant metal polymer interfaces, Progr. Org, Coatings 1998;34:1-12.

[13] Hill D, Holliman PJ, McGettrick J, Searle J, Chatterjee P, Watson TM, Worsley D. Studies of inherent lubricity coatings for lo surface roughness galvanized steel for automotive applications, Lubrication Science 2017; DOI: 10.1002/ls.1370.

[14] Andrews B, Almahdali S, James K, Ly S, Crowder KN. Copper oxide surfaces modified by alkylphosphonic acids with terminal pyridyl-based ligands as a platform for supported catalysis, Polyhedron 2016;114:360-369.

[15] Adden N, Gamble LJ, Castner DG, Hoffman A, Gross G, Menzel H. Phosphonic acid monolayers for binding bioactive molecules to titanium surfaces, Langmuir 2016;22;8197-8204.

[16] Gawalt ES, Avaltroni MJ, Koch N, Schwartz J. Self-assembly and bonding of alkanephosphonic acids on the native oxide surface of titanium, Langmuir 2001;17:5736-5738.

prepare titanium oxide films, Thin Solid Films 2013;548:34–39.

[19] Cordeiro D, Vasconcelos L, Costa VC, Nunes EHM, Sabioni ACS, Gasparon M, Vasconcelos WL. Infrared Spectroscopy of Titania Sol-Gel Coatings on 316L Stainless Steel, Mater. Sci. Appl. 2011;2:1375-1382.

[20] Zhang C, Luo Y, Chen X, Ou-Yang W, Chen Y, Sun Z, Huang S. Influence of different TiO_2 blocking films on the photovoltaic performance of perovskite solar cells, Appl. Surf. Sci. 2016;388:82-88.

[21] Roizard X, Heindrichs J, Borgeot M, Buteri A, Jacobson S, Borgeot M, Carpentier L, Melot JM, Lallemand F. Friction behavior of ferritic stainless steel in a strongly diluted alcohol solution of alkylphosphonic acid, Trib. Int. 2017; DOI 10.1016/j.triboint.2017.04.027.

[22] Trzepiecinski T, Bazan A, Lemu HG. Frictional characteristics of steel sheets used in the automotive industry, Int. J. Automotive Tech. 2015;16:849-863.

[23] Wan Y, Wang Y, Zhang Q, Wang Z, Xu Z, Liu C, Zhan J. Enhanced tribology durability of a self-assembled monolayer of alkylphosphonic acid on a textured copper substrate, Appl. Surf. Sci. 2012;259:147-152.

[24] Lio A, Charych DH, Salmeron M. Comparative Atomic Force Microscopy Study of the Chain Length Dependence of Frictional Properties of Alkanethiols on Gold and Alkylsilanes on Mica, J. Phys. Chem. B 1997;101:3800-3805.

[25] van der Linde G. Predicting galling behavior in deep drawing processes, PhD thesis, University of Twente, Enschede, the Netherlands: 2011. p. 3.

[26] Wapner K, Stratmann M, Grundmeier G. Structure and stability of adhesion promoting aminopropyl phosphonate layers at polymer/aluminium oxide interfaces, Int. J.

5413–5424.

[28] Lebrini M, Fontaine G, Gengembre L, Traisnel M, Lerasle O, Genet N. Corrosion behaviour of galvanized steel and electroplating steel in aqueous solution: AC impedance study and XPS, Appl. Surf. Sci. 2008;254:6943–6947.

[29] Arenas MA, Garcia I, Damborenea J. X-ray photoelectron spectroscopy study of the corrosion behaviour of galvanised steel implanted with rare earths, Corrosion Sci. 2004;46;1033–1049.

[30] Pazokifard S, Farrokhpay S, Mirabedini M, Esfandeh M. Surface treatment of TiO_2 nanoparticles via sol–gel method: Effect of silane type on hydrophobicity of the nanoparticles, Progr. Org. Coatings 2015;87;36–44.

[31] Al-Kandari H, Mohamed AM, Al-Kharafi F, Katrib A, XPS-UPS, ISS characterization studies and the effect of Pt and K addition on the catalytic properties of $MoO_{2-x}(OH)_y$ deposited on TiO_2, J. Electron Spec. Related Phenom. 2011;184:472–478.

[32] Kruse N, Chenakin S. XPS characterization of Au/TiO_2 catalysts: Binding energy assessment and irradiation effects, Appl. Catal. A: Gen. 2011;391:367–376.

[33] Branch B, Dubey M, Anderson AS, Artyushkova K, Baldwin JK, Petsev D, Dattelbaum AM. Investigating phosphonate monolayer stability on ALD oxide surfaces, Appl. Surf. Sci. 2014;288:98–108.

[34] Seah MP, Dench WA. Quantitative electron spectroscopy of surfaces: A standard database for electron inelastic mean free paths in solids, Surf. Interface Anal. 1979;1:2-11.

[36] Sauthiera G, Segurac JJ, Fraxedasa J, Verdaguer A. Hydrophobic coating of mica by stearic acid vapor deposition, Colloids Surf. A: Physicochem. Eng. Aspects 2014;443:331-337.

[37] Nuzzo RG, Allara DL. Adsorption of bifunctional organic disulfides on gold surfaces, J. Am. Chem. Soc. 1983;105:4481-4483.

List of Figures

Fig. 1 (a) Coefficients of friction (μ) *versus* distance for DX56 (red), TiO_2-coated DX56 (grey) and acetone-rinsed **R8-P** (yellow), **R12-P** (purple) and **R18-P** (blue) and (b) mean μ data showing errors. Lighter shading denotes as deposited and darker shading denotes acetone-rinsed data.

Fig. 2 Confocal micrographs of DX56 (a) before LFT and (b) after LFT and (c) **R12-P** coating after LFT and (d) surface topography line profiles of DX56 (i) before and (ii) after 10 LFT passes; **R8-P** (iii) before and (iv) after 10 LFT passes; **R12-P** (v) before and (vi) after 10 LFT passes and **R18-P** (vii) before and (viii) after 10 LFT passes

Fig. 3 (a) Multi-pass LFT of uncoated DX56 (red), **R12-P** coated DX56 (blue) and acetone-rinsed **R12-P** (green) after one, five, and ten LFT passes, (b) images of LFT flat tools (i) before and (ii) after ten passes of LFT with uncoated DX56 showing zinc flake at I, and (iii) after contact with R12-P coated DX56 after ten passes of LFT, and confocal micrographs after 10 LFT passes of (c) uncoated DX56, (d) **R12-P** and (e) acetone-rinsed **R12-P**.

Fig. 4 IR spectra of the **R12-P** coating (a) after deposition and then aged for (b) 3d or (c) 7d. ● υ C-H, ♣ δ $CH_{2sciss.}$, ▼ υ P=O, † υ P-O, γ δ O-H, β υ P-C, α δ $CH_{2\ rock}$.

Fig. 6 (a) mean WCA data for the DX56, TiO_2-coated DX56, **R8-P**, **R12-P** and **R18-P** (light shading = as deposited, dark shading = acetone rinsed) and WCA images for R12-P (b) as deposited, (c) after 3d and (d) after 21d.

Figure 1

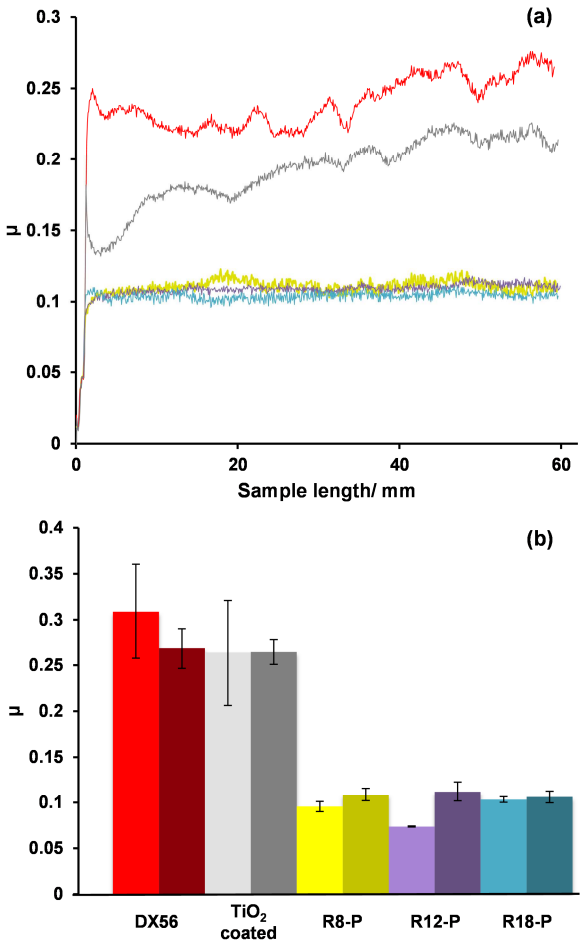

Figure 2

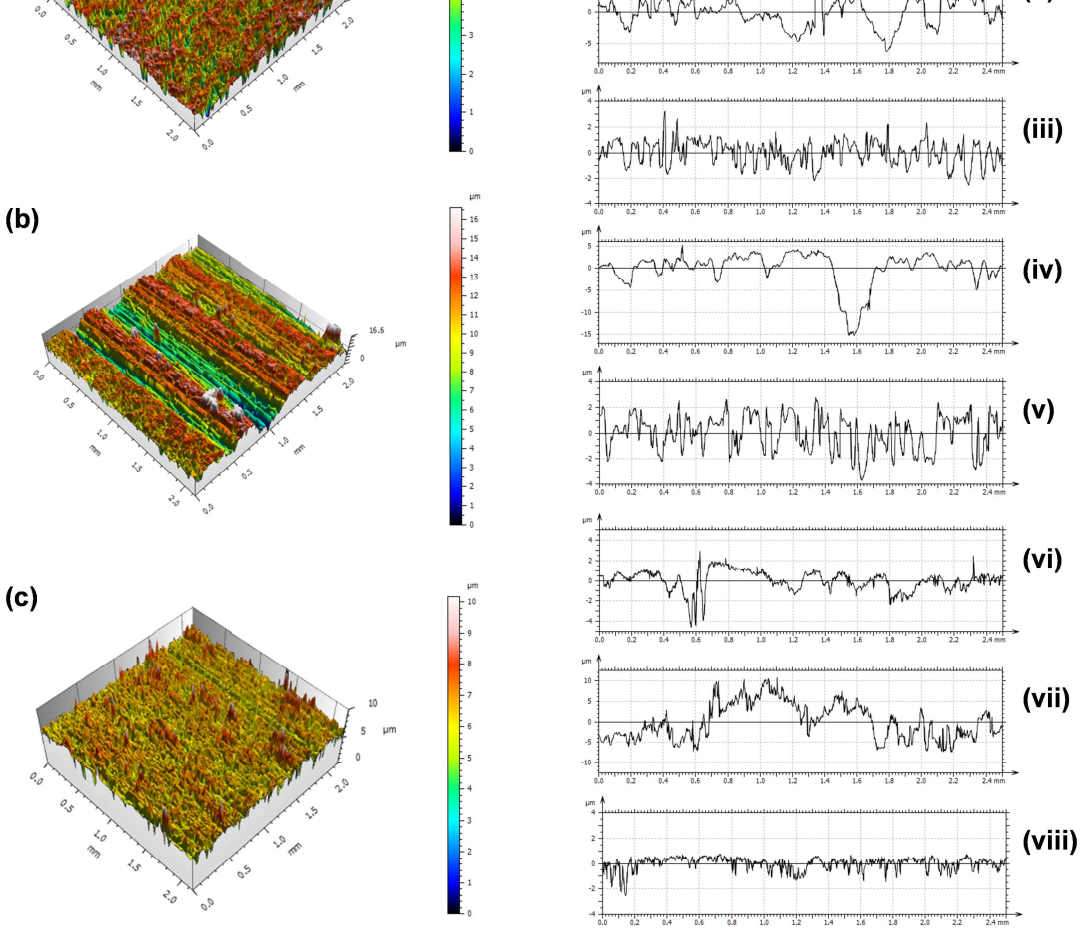

Figure 3

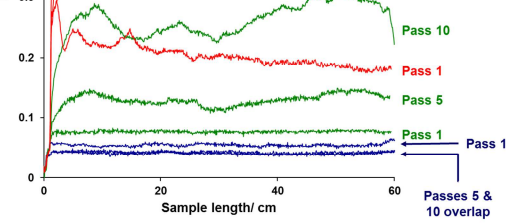

(b)

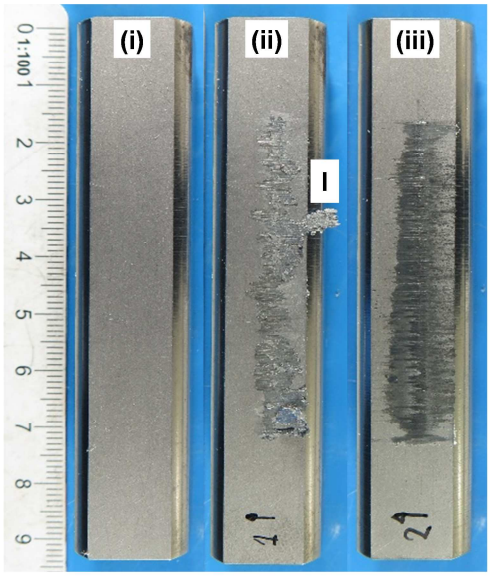

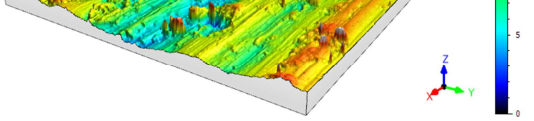

(d)

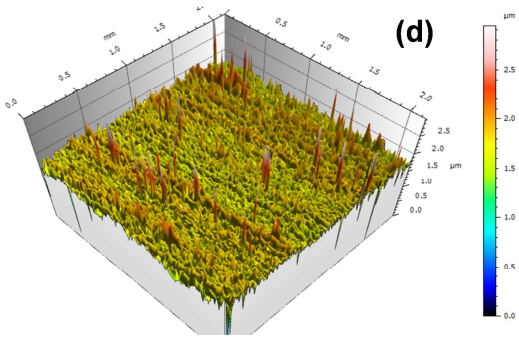

(e)

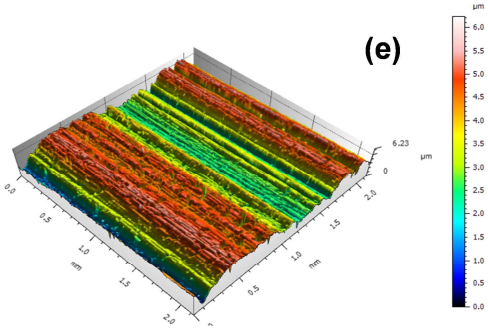

Figure 4

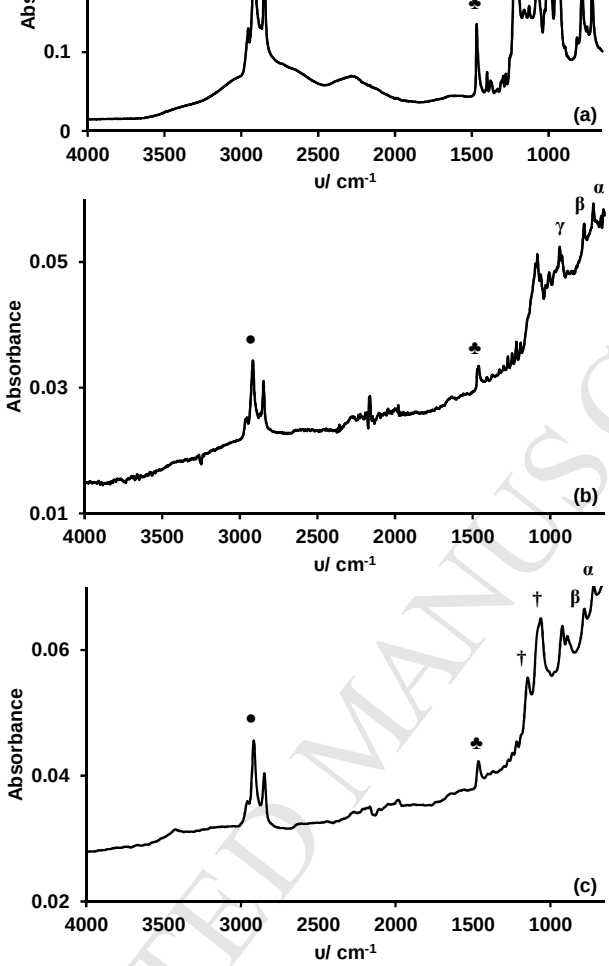

Figure 5

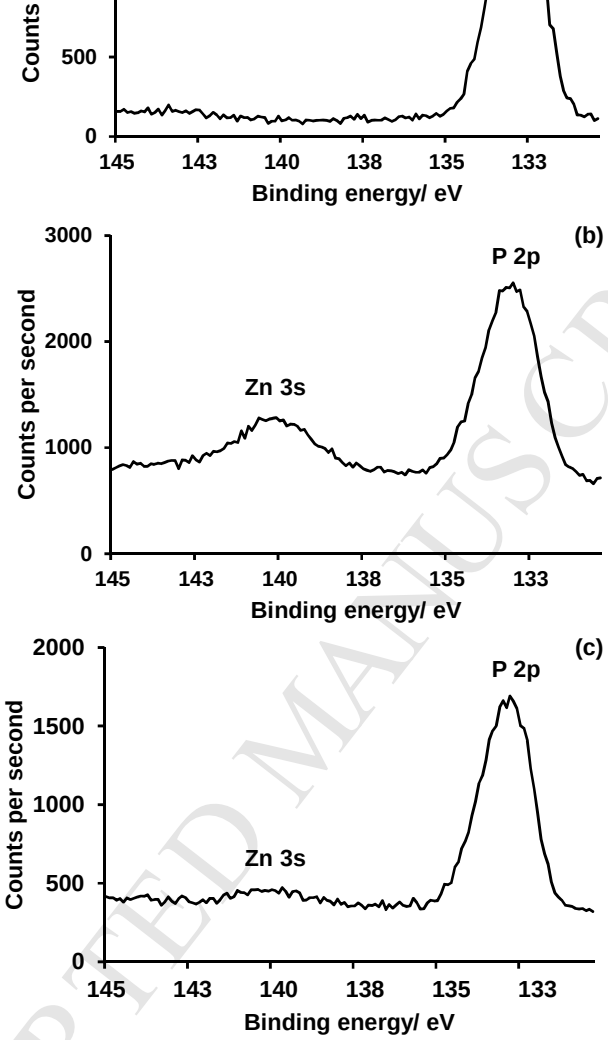

Figure 6

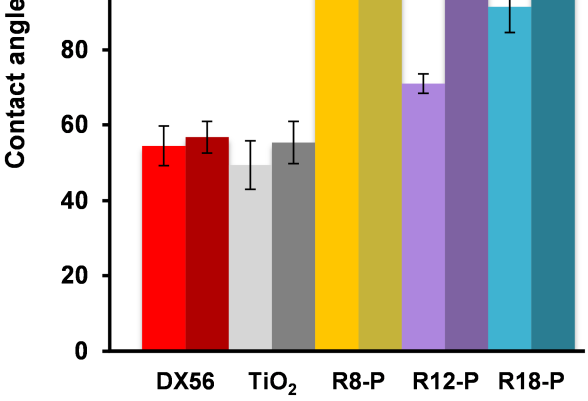

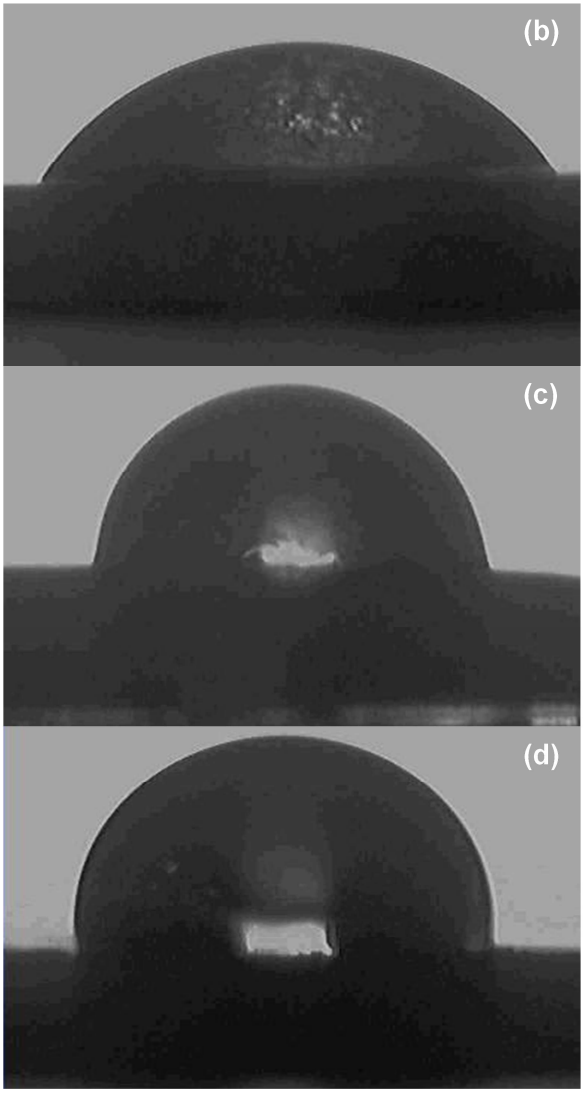

galvanized steel

Donald Hill, Peter J. Holliman, James McGettrick, Marco Appelman, Pranesh Chatterjee, Trystan M. Watson and David Worsley

- the first report of tribological testing of alkylphosphonate coatings on automotive steel
- the first example of tribological and chemical properties changing with sample age
- detailed tribological and characterisation studies of the difference between physisorbed and chemisorbed coatings
- detailed tribological testing of self-assembled coatings using multiple-pass linear friction testing
- studies of the link between tribological performance and water contact angle as a means to accelerate tribological screening